

RESEARCH PROJECT IN MECHATRONICS ENGINEERING

**Soft Robotic Mattress
for Pressure Ulcer
Prevention and Management**

Daniel Lee

Project Report ME040-2019

Co-worker: Ross Philip

Supervisor: Dr Peter Xu

**Department of Mechanical Engineering
The University of Auckland**

27 September 2019

SOFT ROBOTIC MATTRESS FOR PRESSURE ULCER PREVENTION AND MANAGEMENT

Daniel Lee

ABSTRACT

Pressure ulcers are a high cost preventable medical condition that develops after prolonged pressure exposure. Current standard treatment methods are labour intensive and are unable to predict formation without consistent physical examinations. Patients who are bedridden, due to a lack of mobility or a sustained coma, are particularly susceptible to the developing life threatening cases. With US expenditure being upward of \$11 billion annually, there is a high demand for technological solutions for treatment.

Various existing products aim to assist in the management and prevention of pressure ulcers with cyclic surface profiles that regularly redistribute pressure, and pressure mapping mats that can preemptively predict their formation. The following report follows the development of a treatment system that incorporates both actuation and sensing components, integrated to provide continuous pressure redistribution adjustments to achieve an optimal surface profile.

A peristaltic table was repurposed to provide a soft robotic surface which can create custom mattress profiles. A 4×5 array of piezoresistive sensors suspended in a stretchable and flexible elastomer accurately measure the applied force at 20 nodes across the surface, presenting the pressure distribution. Both open-loop and closed-loop actuation control methods were explored, using the pressure map as feedback to spread high loading points to surround areas, ultimately reducing the applied pressure. An operating interface allows for operation of the system with little training and understanding of the underlying technology.

The performance of the system was assessed using a scale test mannequin representing a portion of the human body to apply a realistic pressure distribution expected in clinical situations. Various controller gains were explored to optimise the performance in reducing the maximum pressure on the surface. Reductions of up to 81% were achieved, which would drastically lower the rate of pressure ulcer development.

DECLARATION

Student

I hereby declare that:

1. This report is the result of the final year project work carried out by my project partner (see cover page) and I under the guidance of our supervisor (see cover page) in the 2019 academic year at the Department of Mechanical Engineering, Faculty of Engineering, University of Auckland.
2. This report is not the outcome of work done previously.
3. This report is not the outcome of work done in collaboration, except that with a potential project sponsor (if any) as stated in the text.
4. This report is not the same as any report, thesis, conference article or journal paper, or any other publication or unpublished work in any format.

In the case of a continuing project, please state clearly what has been developed during the project and what was available from previous year(s):

Actuation system was repurposed from a peristaltic tube developed by a masters student.

Signature:



Date:

27/09/2019

Supervisor

I confirm that the project work undertaken by this student in the 2019 academic year is / is not (strikethrough as appropriate) part of a continuing project, components of which have been completed previously. Comments, if any:

Signature:



Date:

27/09/2019

Contents

1	Introduction	1
2	Objectives	2
2.1	Work Distribution	2
3	Literature Review	3
3.1	Predicting pressure ulcer formation	3
3.2	Multiplexing Sensory Array	3
3.3	Intelligent Seat for Alleviating Pressure Ulcers	4
4	Actuation System	5
4.1	Overview	5
4.2	Change Summary	6
5	Sensing System	6
5.1	Sensor Selection	6
5.2	Sensing Interface Selection	7
5.3	Array Construction	8
5.3.1	Performance Testing	8
5.4	Simulation Verification	9
5.4.1	Molding Process	9
5.5	Interfacing to the Microcontroller	10
5.6	PCB Design	10
5.6.1	Schematic Design	10
5.6.2	Board Development	11
5.7	Microcontroller Sampling	11
5.8	Sensor Calibration	11
6	Operating Interface	12
6.1	Communication	13
6.2	GUI	13
7	Control Logic	13
7.1	Open Loop Control	14
7.2	Closed Loop Control	14
7.2.1	Average	14
7.2.2	Localised Average	15

8 System Testing	15
8.1 Test Mannequin	15
8.2 Open Loop Control	16
8.2.1 Methodology	16
8.2.2 Results	16
8.2.3 Discussion Open-loop	16
8.3 Closed Loop	17
8.3.1 Methodology	17
8.3.2 Results	17
8.4 Discussion - Average Controller	18
8.5 Discussion - Localised Average Controller	18
8.6 Discussion - General Closed-loop	18
9 Conclusions	19
10 Recommendations for Future Work	19
References	20
Appendix A: Arduino Loop Function	21
Appendix B: Localised Average Controller Function	22
Appendix C: Altium PCB Schematic	23

List of Figures

1 Alternating pressure air mattress, from Vitality Medical	1
2 Pressure mapping device [6]	1
3 Proposed modification to the Reswick and Rogers pressure time curve [8] . . .	3
4 Tyre Pressure Image [9]	3
5 Sensor arrangement [9]	3
6 Intelligent Seat Sensing Array	4
7 Repurposed Peristaltic Table Design	5
8 Model Visualisation	6
9 Simscape Actuation System Module	6
10 Surface deformation [1]	6
11 Flexiforce A401 Sensor [13]	7
12 Tekscan Flexiforce A401 Interfacing Circuits	7

13	Tekscan Flexiforce A401 Interfacing Circuit Performances	8
14	Flexiforce A401 sensor suspended in Ecoflex™ 00-30	8
15	Sensing Calibration	9
16	Interface Schematic	9
17	Molding Process	9
18	Ecoflex™ Sensing Array	10
19	Multiplexer Schematic	10
20	Linear Regulator Schematic	11
21	Altium PCB Design	11
22	Sensor Calibration: Pressure vs Voltage Relationship	12
23	Soft Robotic Diagram Data Flow Diagram	12
24	Operating System GUI	13
25	Average Controller Block Diagram	14
26	Sensing Array Distance Propagation	15
27	Mannequin	16
28	Pressure Distributions for Lines Method	16
29	Pressure Distributions for Diamond/Checker Method	16
30	Test Arrangement	17
31	Maximum Pressure Reduction over Time	17
32	Actuation and Surface Profile Development for Localised Average Control	18

Acknowledgements

I would like to thank the following people for their supporting contributions in ensuring the successful progression of this research project:

Peter Xu, project supervisor, for overseeing the development and research of this project, sharing your knowledge and experience when it came to making design decisions.

Ross Philip, project partner, without such a cohesive co-worker with a strong dedication and sewing skills, the project would not have progressed as far as it did.

Marshall Lim, lab technician, for assisting in the PCB development process and procuring the manufacturing process and all necessary components. Your technical mastery lifted the quality of work behind the final product, resulting in a system I could be proud of.

Emanuele Romano, lab technician, who generously assisted in the use of the acrylic cutting and engraving machine. Without you, the project would lack the token covering plaque.

Logan Stuart, lab technician, for your expertise in 3D printing and providing a great working environment.

Definitions

- **Sensel:** A single sensor element of an array of sensors
- **Necrosis:** Premature death of cells in living tissue
- **Sacral:** Region surrounding the first two vertebrae on the lower back
- **Peristaltic:** Wavelike muscular contractions
- **Piezoresistive:** A change in electrical resistance when mechanical strain is applied

Abbreviations

- **ADC:** Analog-to-Digital Converter
- **APAM:** Alternating Pressure Air Mattress
- **GUI:** Graphical User Interface
- **PCB:** Printed Circuit Board
- **SPI:** Serial Peripheral Interface
- **UI:** User Interface
- **USB:** Universal Serial Bus
- **UX:** User Experience

Nomenclature

D	Distance between actuating node and sample node
D_L	Distance limit defining the surround nodes to sample
D_s	Distance scalar defining the diminishing influence of surrounding samples
K	Proportional controller gain
N_{ij}	Actuation node at position (i,j) in actuation array
S_{kl}	Sample at coordinates (k,l) from the sensory array

1 Introduction

Pressure ulcers, more commonly known as 'bed sores' are a preventable condition that affects soft tissue after prolonged pressure is applied to the skin. They result in the discolouration and bruising in mild cases and necrosis of skin and underlying cells in more severe conditions [1]. Health care centers across Europe recorded a prevalence in over 10% of admitted patients, with 59% developing the condition during their care [2]. Elderly, ill and comatose patients are particularly susceptible to the condition, due to a lack of pain recognition and mobility.

The current standard treatment for pressure ulcers involves regular manual re-positioning of patients and applying moisturiser to the affected areas. These labour heavy practises result in high costs, with the US health care expenditure being estimated upward of \$11 billion per year alone [3]. Since hospitals in the US stopped receiving Medicare payments for late stage pressure ulcer injuries in October 2008 [4], there has been a growing demand for autonomous prevention treatment options.

Alternating pressure air mattresses (APAMs) are a currently available market product that aims to reduce the risk of pressure ulcer formation, by providing cyclic redistribution of pressure. This is commonly achieved through an array of air pockets which are inflated and deflated to provide varying patterns that shift loading points on the patient. An example is demonstrated in Figure 1, showing a typical grid arrangement alongside the air control unit.

Random control trials on the effectiveness of APAM's found them to be effective in reducing the formation of heel ulcers, however, saw an increase in sacral ulcers for more susceptible patients relative to the control [5].

Inconsistencies in the performance of these cyclic systems is motivating research into more personalised solutions that aim to better redistribute pressure for specific patient conditions.



Figure 1: Alternating pressure air mattress, from Vitality Medical



Figure 2: Pressure mapping device [6]

Other pressure ulcer prevention approaches have involved the use of continuous bedside pressure mapping (CBPM) devices, shown in Figure 2. These provide a real-time display of pressure distributions. Trials conducted on hospital patients saw a significant reduction in the formation of pressure ulcers when nurses moving patients were assisted by a CBPM system [6].

The aim of this project is to develop a system that incorporates both actuation and sensing components to provide real-time pressure redistribution. Ultimately preventing the development of pressure ulcers by shifting high loading points to surrounding areas that can bear the load.

The following report documents the research and development process that went into the development of a working scale prototype, with a particular focus on the pressure mapping and automated feedback control. For a more extensive discussion on the actuation system and operating interface, please review the supporting paper completed by Philip [7].

2 Objectives

The development of a successful pressure ulcer prevention system will involve each section to be purpose built for the specific application. Individual objectives have been outlined below with their primary requirements:

- **Actuation System:** Develop an array of actuators that can vary the elevation of various points on the bed, ultimately redistributing the pressure experienced by the patient. In support, a range of actuation systems will be explored to evaluate their ability to redistribute pressure and manage micro-climate factors.
- **Pressure Mapping:** Accurately record and process the interfacing pressure distribution imposed on the patient. Requiring a pressure sensing array and interface to accurately monitor the interface between the bed and skin of the patient. The viability of various pressure mapping methods will be explored given the application and development constraints.
- **Operational Interface:** Create an interface and control capabilities that allow for intuitive operation of the system. Developing a graphical user interface that allows nurses, doctors, or hospital staff to observe pressure mapping information and make appropriate actuation adjustments on the bed surface. The system will aim to be robust to user error while maintaining clear and comprehensive usability.
- **Automatic Control:** Integrate control methods to automatically adjust the surface profile to reduce the need for human interaction in the treatment process. Both open-loop and closed-loop techniques will be explored, utilising the information received from the sensory array as a form of feedback. This aims to automate the adjustment process on the actuation system to redistribute the pressure on the mattress in real-time. The aim for this section is to ultimately improve the treatment response time and reducing the dependency of nurse and doctors.

2.1 Work Distribution

As part of this project, work was distributed with my co-worker Philip. To specialise the contributions towards the development of the robotic mattress, Philip's work primarily focused on the development of the actuation and operation interface. While work and research outlined in this report concentrates on the creating of the pressure mapping and closed-loop control, an in-depth discussion on other portions of the development process can be found on Phillip's paper [7].

3 Literature Review

Before committing to the design and construction of the cohesive system, research was conducted to explore relevant studies and technologies to support development decisions.

3.1 Predicting pressure ulcer formation

Reswick and Roger's curve is a tool used for assessing the risk of developing pressure ulcers [8]. The curve demonstrates the relationship between pressure intensity and length of exposure at which pressure ulcers are likely to form. The original function proposed for a general prediction is as follows:

$$P = \frac{40kPa}{t} \quad \text{where } t \text{ is the exposure time (hours)} \quad (1)$$

However, recent revisions of the model suggest modifications at the extremities of the prediction curve. This follows clinical trials demonstrating the development of pressure ulcers in short duration's when exposed at medium-high pressure [1]. The original and proposed curves can be seen in Figure 3.

Because patients that are subject to hospital beds are likely to be left unattended for extended periods of time, the system aims to focus on exposure times between one and eight hours. Considering the Reswick and Rogers relationship, pressures ranges of 5-40kPa are a potential risk at developing pressure ulcers at these exposure levels. Therefore, the pressure mapping system resolution should accurately represent these values.

3.2 Multiplexing Sensory Array

The construction of large area flexible sensors have been explored which utilized screen printing techniques, along with piezoresistive materials to create high resolution pressure mapping, as demonstrated in Figure 4 [9]. A Ag-filled polymer is traced in parallel lines onto thermoplastic sheets to create a conductive interface. Within the sensing area, the conductive tracers are then covered by a semi-conductive ink. Two printed thermoplastic sheets are combined together to form a grid of semi-conductive separated traces, as shown in Figure 5. Intersections of the grid act as piezoresistive interfaces, where the conductivity will vary with an applied perpendicular force, ultimately creating a large scale array of sensors.

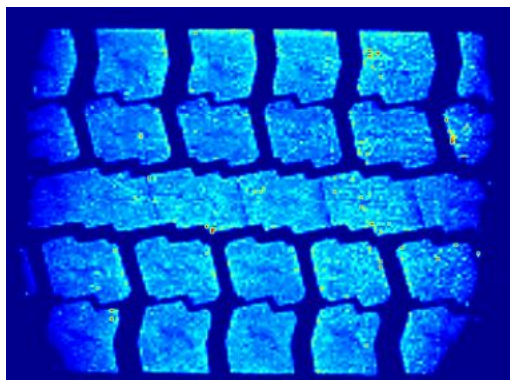


Figure 4: Tyre Pressure Image [9]

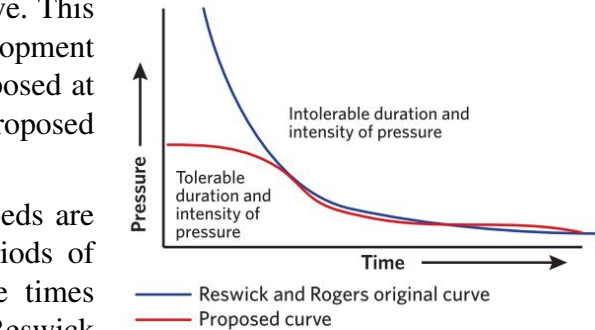


Figure 3: Proposed modification to the Reswick and Rogers pressure time curve [8]

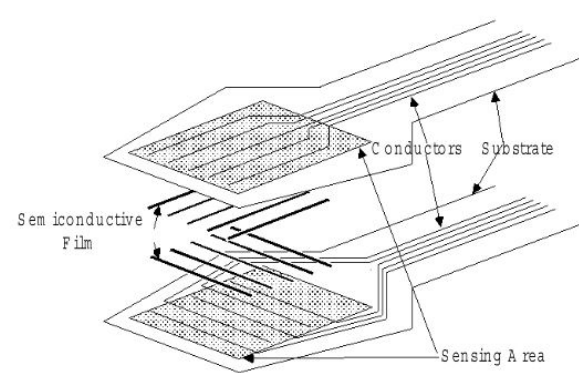


Figure 5: Sensor arrangement [9]

Given the grid arrangement of connections, sensels are unable to be sampled simultaneously, therefore, an analogue multiplexing circuit is implemented to sample individual elements using a switching drive and sense address to feed into a single interfacing ADC. This system is advantageous as it reduces the number of op-amps required for the array, reducing the number of components required from $N_{rows} \cdot N_{column}$ to N_{rows} where N is the number of conductive traces. Additionally, the multiplexing system drastically reduces the number of ADC interfaces required for the circuit, reducing from $N_{rows} \cdot N_{column}$ down to 1. However, this limits the sampling rate for sensels within the array as readings have to made individually.

Performance of such an array proved to be very effective in mapping large areas at a sufficient sampling rate, making it potentially suitable in the application of body pressure mapping for pressure ulcers. System hardware used allowed for a 52×44 array, sampling at 225Hz, with a resolution of 250 sensels/cm² possible with high accuracy screen printing.

Unfortunately, quotes requested for such sensing systems far exceeded the budget of this research, ranging from \$5,000 to \$10,000. However, the idea of utilizing multiplexing for the system interface could be useful in the subsequent sensing array signal processing design.

3.3 Intelligent Seat for Alleviating Pressure Ulcers

A recent paper explored the development of an intelligent seat that aims to sense and redistribute pressure, with a focus on seniors and elders residing in nursing homes [10]. The systems pressure mapping component consists of a sensing array using 16 piezoresistive sensors, which are secured onto a thin plastic sheet. These are processed using an Arduino ATmega 2560 board, after the sensor resistance is converted into an intelligible voltage, which is demonstrated in Figure 6.



Figure 6: Intelligent Seat Sensing Array

The plastic sheet offers a stable surface to maintain the position of each sensel, however, the material provides minimal stretching. Therefore, when the surface is deformed significantly to redistribute the pressure across the surface of the seat, the position of surrounding sensors is shifted. Because this movement is not accounted for in the processing stage of the pressure mapping process, the pressure distribution data is skewed and is no longer an accurate representation.

4 Actuation System

4.1 Overview

The actuation system has been repurposed from a peristaltic table developed by a masters student (Hashem.R) at the University of Auckland [11]. The system originally aimed to move organic matter for use in production lines using a soft deformable surface made from the flexible silicone substrate material Ecoflex™ 00-30. Changes in the actuation control methods enabled the surface to be conformed into surface profiles to distribute surface pressure.

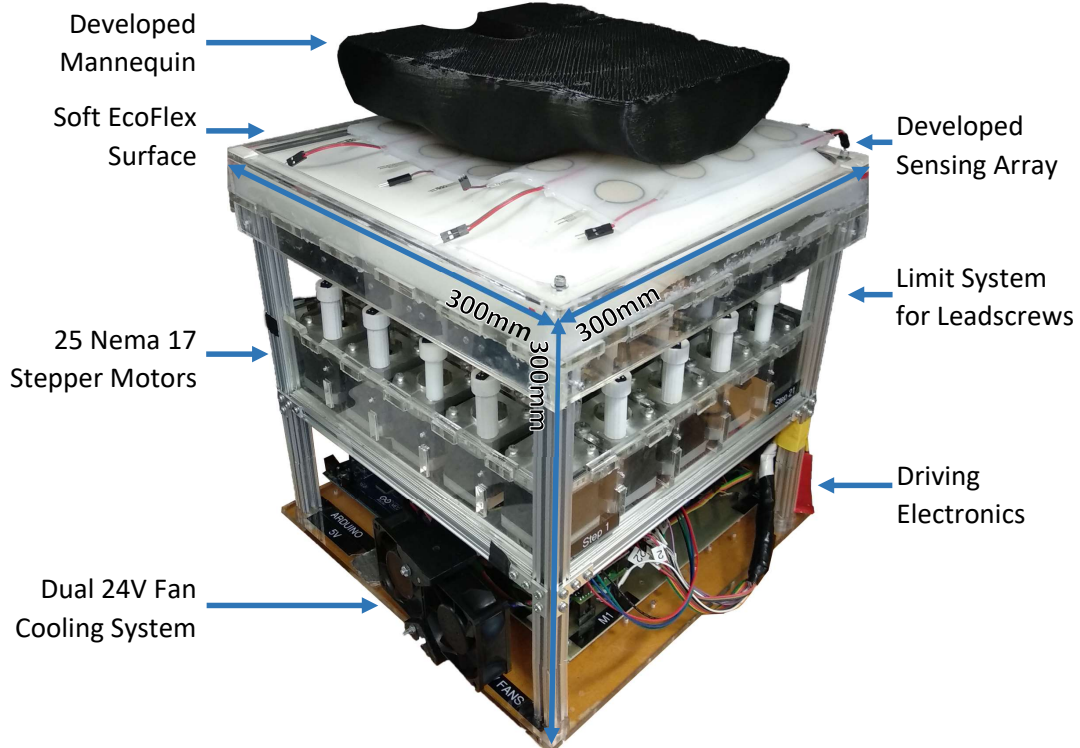


Figure 7: Repurposed Peristaltic Table Design

Figure 7 demonstrates a summary of the key components to the actuation system. Surface deformation is controlled by a series of linear actuating washers embedded in the rubbery surface. The linear motion of each washer is sourced by a Nema 17 stepper motor with a lead screw actuator. The 4×5 array of actuating modules enables the formation of complex pattern on the surface to heights of 30mm. The soft surface flexible and stretchable surface enables the distribution of pressure for objects or patients resting above. The system benefits from the advantages of rigid robotics, with high precision and repeatability from the stepper motors. As well as soft robotics, with an ergonomic interface that can mold to complex surface patterns. Ultimately fulfilling the requirements for the actuation system desired for the soft robotic mattress.

To control the height of each individual stepper motor, a purpose built microcontroller utilising an EasyDriver v4.4 was used to convert a desired height into an appropriate PWM signal. A limit switch positioned at the base of each lead screw provides a zeroing position for each of the actuators, while preventing the modules from over running. Desired actuator heights are controlled by an Arduino ATmega 2560 board, with the information being transmitted to each individual microcontroller via SPI protocol.

4.2 Change Summary

The repurposing process involved a series of adjustments and repairs to the actuation system developed in 2015 to get the system back into a state of consistent operation. Key changes are discussed in depth in Philip's report [7] and summarised below:

- **Stepper Motor Controllers:** While inspecting the electronics in the inherited control system, four of the stepper motor controllers had obtained irreversible damage and were no longer operable. Due to limited development time for the project, a decision was made to utilise 20 of the working modules to operate a 4×5 array of actuators.
- **Limit Switch Overhaul:** An initial assessment of the limit switches revealed a large portion of the 3D printed supports had been previously damaged. Instead of replacing them with the same parts, the design was improved to strengthen the structural integrity in the hopes of preventing similar damage. While replacing printed parts, the electrical limit switch connections were repaired to create more robust transmission lines.
- **Cooling Fan Relocation:** Heat produced by the actuation electronics would cause the stepper motor controls to overheat during extended run times. A mount was developed to support a dual 24V DC cooling fan arrangement, positioned to provide an optimal distribution of forced convection air cooling.
- **Simscape Modelling:** A simulation of the actuation system was modelled in the Matlab Simulink extension Simscape to provide a virtual visualisation of the deformable surface (Figure 8). Additionally, the model enables a force analysis for each of the 20 modules. The block diagram for an individual actuation system module can be seen in Figure 9.

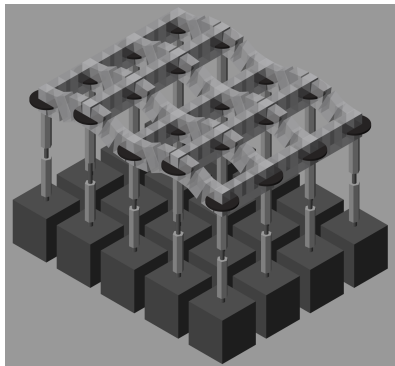


Figure 8: Model Visualisation

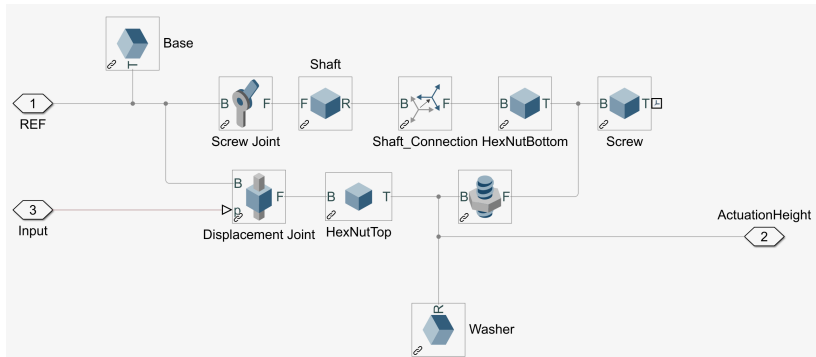


Figure 9: Simscape Actuation System Module

5 Sensing System

5.1 Sensor Selection

Strain gauges were explored for their use in identifying the deformation of the soft Ecoflex™ surface, due to an applied pressure. Similar to the way the strain of tissue is represented in Figure 10, as a result of imposed stresses from the applied pressure. However, due to the nature of the actuation system, the movement of the surface would result in the stretching of the soft rubber and provide undesirable disturbances to the strain gauge's variable resistance.

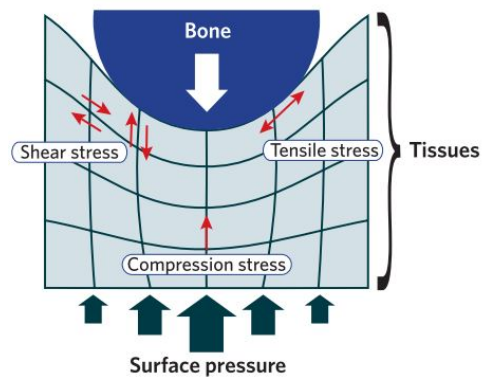


Figure 10: Surface deformation [1]

Piezoresistive materials are a common choice of sensor technology for pressure sensing applications [10, 9]. They utilize a semi-conductive layer suspended between two conductive terminals that have a resistance proportional to the loading pressure. Relative to alternative flexible tactile sensors, they offer high sensitivity and repeatability. With their fragile mechanical properties can be protected by elastomers to prevent direct contact [12].

High density piezoresistive pressure sensing arrays are available, as discussed in the literature review section 3.2. These can provide a high resolution pressure map, however, the technology exceeded the budget of this project. Therefore, a sensing array utilizing multiple piezoresistive sensors was developed.

The Flexi-force A401 [13] was chosen for the development of the sensing array, as shown in Figure 11. This sensor provided a base force range of $0 - 111N$ across a $506mm^2$ area, resulting in a $219kPa$ pressure capacity.

$$P = \frac{F}{A} = \frac{111}{(0.0254)^2 \pi} = 219kPa \quad (2)$$

With the focus of pressure reduction in a range of $5 - 40kPa$, as outlined in section 3.1, the Flexiforce A401 has the capacity to map pressures likely to form pressure ulcers. In addition, the large sensing area provides a good coverage of the surface without the need for high resolution array.

To ensure the resolution of the pressure mapping had sufficient feedback for the development of a redistribution control, 20 sensels were arranged to provide a sensory input for each actuator. This enables pressure readings to be made at the locations on the mattress that are able to be directly deformed, allowing for more accurate pressure loading management.

5.2 Sensing Interface Selection

To sample the loading on an individual sensor, an interfacing circuit needs to be used to convert the variable resistance to an intelligible voltage. Documentation provided by the manufacturer [14] suggested three electrical arrangements when using their A401 sensor, which are demonstrated in Figure 12.

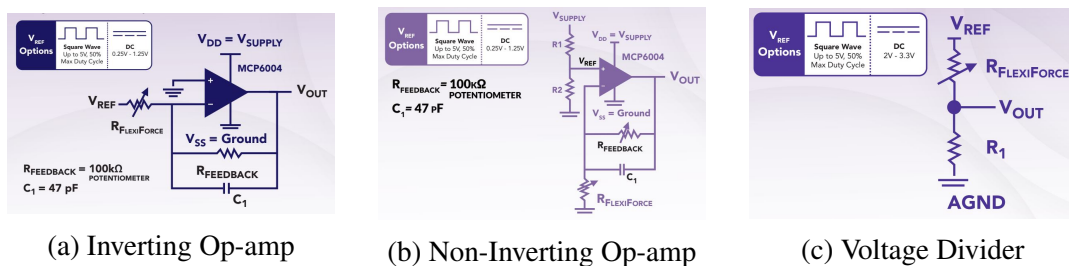


Figure 12: Tekscan Flexiforce A401 Interfacing Circuits

Each arrangement offers a setup of varying complexity, with the inverting op-amp in Figure 12a requiring a dual supply to offer a negative potential reference voltage and the more basic voltage divider in Figure 12c requiring a single source and resistor to operate. The trade off in reduced complexity is a drop in the range of electrical potential from the interface. With the

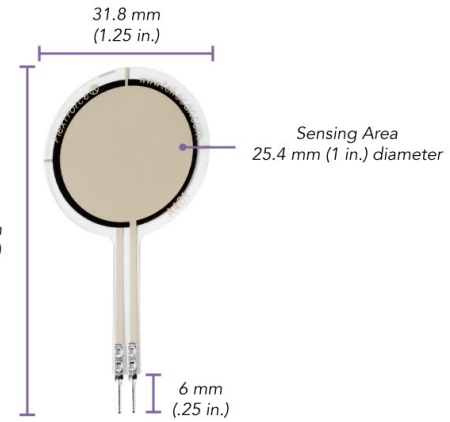


Figure 11: Flexiforce A401 Sensor [13]

ADC's of the microcontroller having a fixed input resolution, as the range in voltage reduces, the utilisation of the ADC's capacity reduces. This in turn reduces the resolution of the sensing interface. The performance capacity of each arrangement is demonstrated in Figure 13.

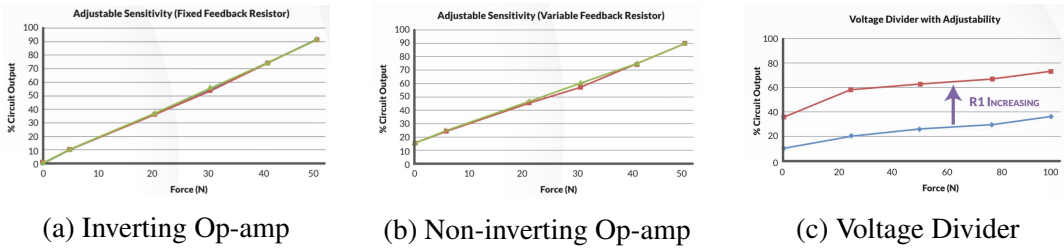


Figure 13: Tekscan Flexiforce A401 Interfacing Circuit Performances

As expected, the Inverting Op-amp (Figure 13a) provides the best performance, utilizing the full 100% of the potential voltage capacity. The Non-inverting Op-amp arrangement (Figure 13b) ranging from 15% to 90% offers 75% of the capacity, while the Voltage Divider method only takes advantage of 35%.

Given the investment into the sensors, using a voltage divider arrangement would have wasted a large portion of their potential (65%) and was therefore not considered as a potential interface. Although, there would have been advantages in utilising the Inverting Op-amp arrangement, sourcing a dual supply for the electrical interface was not practically feasible. This was due to the actuation system already occupying an entire 10A power supply individually. Therefore, the Non-inverting Op-amp arrangement was used.

5.3 Array Construction

With the sensors having been selected, they then needed to be constructed into an array that would be able to maintain their positional arrangement and protect them from potential damage. Patients resting on the mattress will need to be able to move without disturbing the location of the sensors, resulting in abrasive damage that would render inaccuracies in pressure readings. To solve these issues, the array of sensors are suspended between two 2mm layers of Ecoflex™ 00-30, providing both structural support and protection. The additional benefit of utilising the stretchable Ecoflex™, is that it allows for the supporting material to deform with the surface of the bed, allowing sensors to remain in their original position as surrounding areas on the mattress rise and fall.

5.3.1 Performance Testing

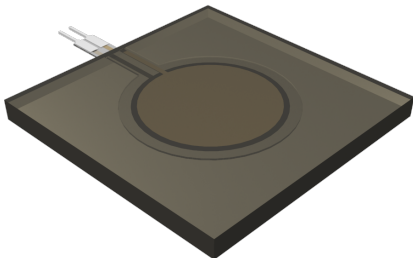


Figure 14: Flexiforce A401 sensor suspended in Ecoflex™ 00-30

Before committing to the Ecoflex™ arrangement described, pressure sensing tests were conducted with a Flexiforce A401 sensor suspended between the two layers. Because the rubbery material is likely to absorb a portion of the pressure loading, the sensors would no longer represent the expected pressure to resistance ratio under standard conditions. The loading absorbed by the compressed Ecoflex™ rubber would not be transferred to the sensing material and therefore provide an underestimation on the true pressure.

A test mold that encapsulated an individual A401 sensor was cut from 2mm thick acrylic to hold the Ecoflex™ while it set from a liquid to solid state and holding the sensor in place. A 3D model of the testing piece can be seen in Figure 14.

The testing procedure involved applying a range of loads to the test piece while it rested on the surface of the actuation system, evaluating the output voltage. Weights ranging from 0 – 5kg were applied perpendicularly to the test piece, as shown in Figure 15. The weights were selected for the given surface area so that the pressure applied would depict that which was likely to form pressure ulcers.

As expected, the range of sensitivity for the piezoresistive sensors was dramatically reduced when encapsulated in the Ecoflex™. Even when loaded at 49N (104kPa), the voltage reading was less than 1V, which was dramatically less than the expected 2-V.

Fortunately, the sensitivity range for the Flexiforce A401 sensors is able to be adjusted by either varying the reference voltage on the non-inverting input or the feedback resistance. Therefore, various feedback resistance values were tested on a breadboard setup until the sensor sensitivity consistently ranged a pressure of 0 – 40kPa. Resulting in a feedback resistance $R_f = 10M\Omega$, demonstrated in Figure 16.

5.4 Simulation Verification

5.4.1 Molding Process

Once the sensing arrangement had been successfully tested and verified, the complete 4×5 array of 20 sensors were ready to be molded into Ecoflex™. Batches of four sensors were completed at a time, forming an entire row with the terminals of the two nearest sensors extending out of each short edge.

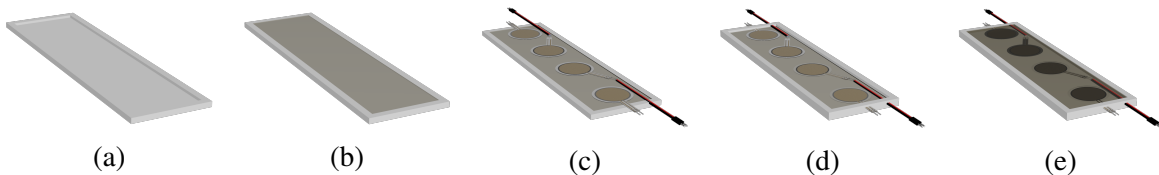


Figure 17: Molding Process

The molding process involved five distinct stages, visually demonstrated in Figure 17:

- (a) Starting base mold is made from laser cut acrylic, forming a $200 \times 50 \times 2\text{mm}$ rectangle
- (b) First layer of Ecoflex™ is poured and sets after 8 hours
- (c) Sensors and wiring are laid out, centered 25mm from each edge and neighbouring sensors
- (d) Placed the second molding layer above and secured using hot glue to prevent leakage
- (e) The final layer of Ecoflex™ is poured and left for 8 hours to set

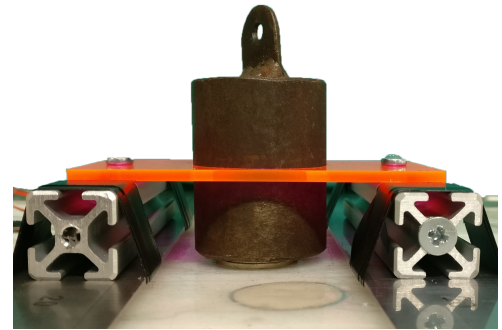


Figure 15: Sensing Calibration

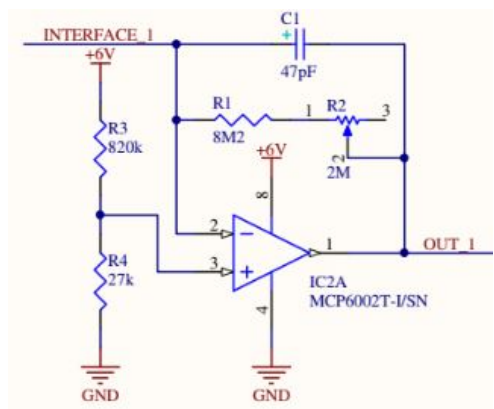


Figure 16: Interface Schematic

Due to the nature of the curing reaction taking place when the Ecoflex™ sets, the top and bottom layers fuse together around the sensors they encapsulate, holding them in place. Following the completion of each of the 5 rows, the strips were then joined together using a mixture of Ecoflex™ that was left to set for 10 minutes, acting as form of binding glue. This produced one cohesive 4mm sheet containing the 20 Flexiforce A401 sensors, shown in Figure 18. This is both flexible and stretchable, allowing it to conform to the surface while maintaining the positions and protecting the sensors.

The array was then attached to the actuation surface using a silicone glue at each actuation point. This ensures the array remained aligned with the actuation system below as a result of the abrasive force of objects or patients resting on the mattress.

5.5 Interfacing to the Microcontroller

To sample and record readings from the 20 Flexi-force A401 sensors, the Arduino mega 2560 microcontroller in the actuation system. This is equipped with 16 ADC's that were not being utilized, which made them a great interface. However, due to the array containing 20 sensors, 16 ADC's would not be enough to sample all of them at once. Therefore, analogue 4:1 multiplexers were used to alternate 4 sensors being fed into an individual interface, reducing the required microcontroller sampling ADC's down to 5.

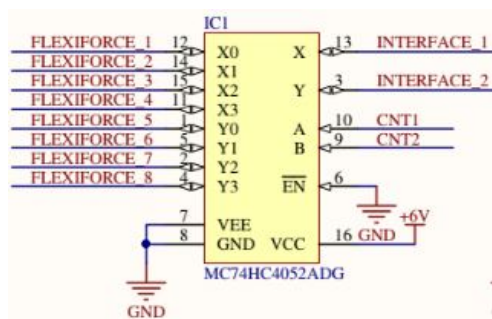


Figure 19: Multiplexer Schematic

A schematic demonstrating the dual 4:1 analogue multiplexing arrangement is shown in Figure 19. The control pins (CNT1, CNT2) were connected to digital output pins on the Arduino ATmega 2560 board. These can be used to determine the current sensors being sampled by each of the two interfaces on the output ports (X, Y). The enable pin (VEE) has been grounded to set the multiplexers into a continuous operation mode. This allows the microcontroller to both record and control samples from the 20 sensors in the pressure mapping sensory array.

5.6 PCB Design

With the circuitry to process the sensory signals growing in complexity, requiring numerous multiplexers and op-amp interfaces, a PCB was developed to miniaturise the design. This provided a more portable and robust solution by maintaining a compact layout.

5.6.1 Schematic Design

The schematic overview of the five sensor interfaces and 4:1 multiplexer sections are demonstrated in Figures 16 and 19. In addition to these portions of the design, both power management and connection points needed to be incorporated to PCB to allow for complete implementation.

The ideal operating power for the op-amp and multiplexers are +6V and the supply voltage used in the actuation system was 24V. Therefore, a linear regulator was selected to step down the potential voltage to avoid damaging the components. The peak power draw for the circuit was experimentally determined to peak at 30mA, therefore, a LM317L regulator was selected.

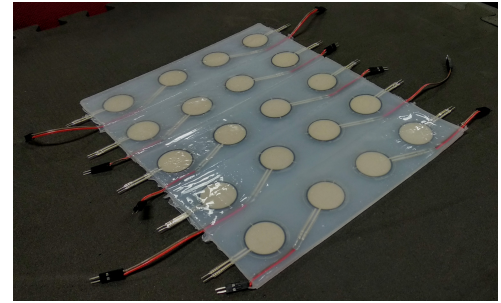


Figure 18: Ecoflex™ Sensing Array

The LM317L is an adjustable regulator which can provide a variable output voltage using a voltage divider. Design processes were provided in the manufacturers datasheet [15] for determining resistor and capacitor values for the design.

$$V_{OUT} = V_{REF}(1 + \frac{R_2}{R_1}) + I_{ADJ}R_2 \quad \text{where } V_{REF} = 1.25V \quad (3)$$

Because in common applications $I_{ADJ} = 50\mu A$, it is negligible in design and therefore ignored. Evaluating this relationship resulted in resistor values for R_1 and R_2 of $27k\Omega$ and $100k\Omega$ respectively, demonstrated in Figure 20.

To allow for the sensor input/output and multiplexer control connections, a series of 2.54mm header pins were incorporated into the board design, which are observable in Figure 21.

5.6.2 Board Development

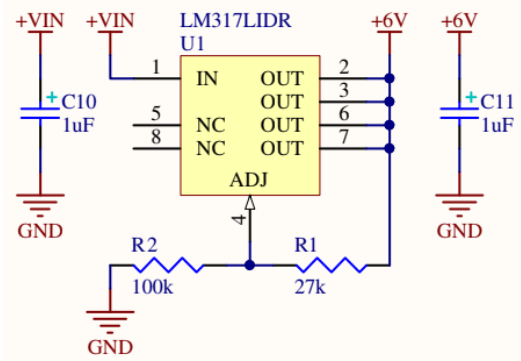


Figure 20: Linear Regulator Schematic

A PCB was arranged to optimally align to best fit the requirement components. Primary connection points are labelled and coloured on a board preview on Altium in Figure 21.

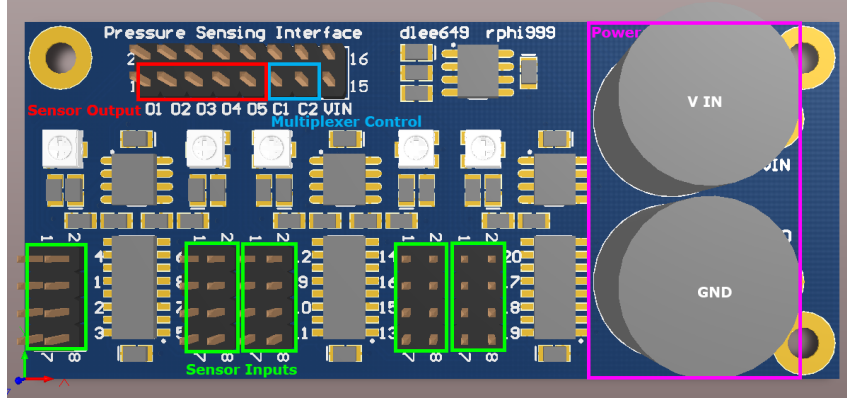


Figure 21: Altium PCB Design

5.7 Microcontroller Sampling

For the Arduino ATmega 2560 microcontroller board to successfully record the pressure mapping sensory array, a script was developed to cycle through the states of the multiplexers while sampling the interfacing voltage. This had to be integrated alongside the actuation system running on the microcontroller chip, and demonstrated in Appendix A.

5.8 Sensor Calibration

To convert the sampled voltage values to an accurate pressure reading that would provide valuable information for assessing pressure ulcer formation, the sensors needed to be individually calibrated. The same testing rig previously used, demonstrated in Figure 15, was utilised to maintain a perpendicular weighted load to each sensor. Voltage readings were recorded for a range of weights ranging from 0-5kg, for each of the twenty sensors to find their Pressure vs Voltage relationship. Weights were converted to pressure by dividing by the Flexiforce A401 sensing area, as demonstrated in equation 4.

$$P = \frac{mg}{A} \quad \text{where } g = 9.81ms^2 \quad \text{and } A = \pi(\frac{25.4}{2})^2 \quad (4)$$

Results from the calibration process are demonstrated in Figure 22, with all the sensors following a similar positive linear relationship as described by the manufacturer in Figure 13.

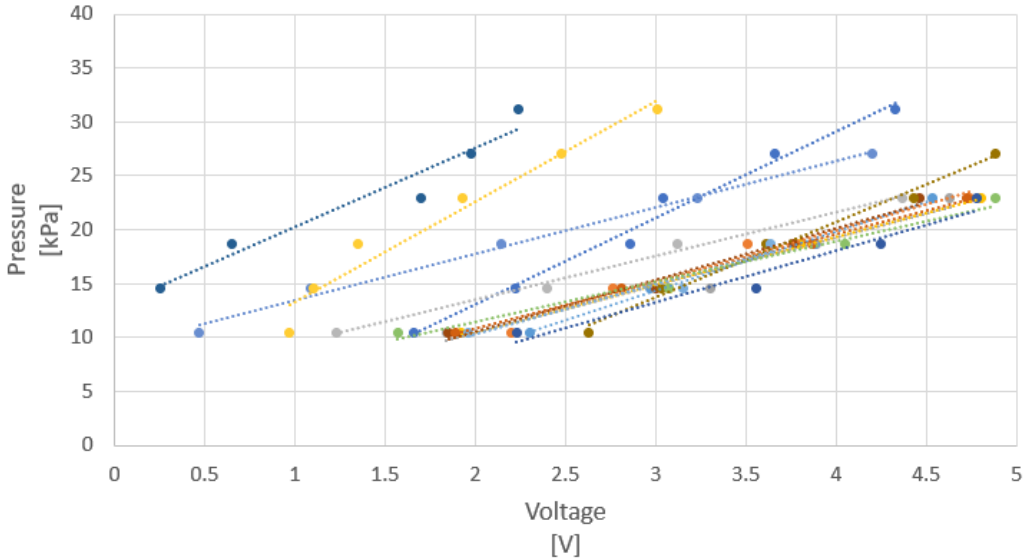


Figure 22: Sensor Calibration: Pressure vs Voltage Relationship

The manufacturer of the Flexiforce A401, Tekscan, lists an acceptance criteria for a $\pm 40\%$ variation between sensor performance outputs. This would justify the differences observed in the trends across the 20 relationships. Linear trendline approximations of the relationships for each individual sensor provided an equation for converting the voltage into pressure. The no load conditions were excluded when forming plots as it acted as a significant outlier for most trend relationships, causing them to skew accurate readings at high pressure loads down. This was deemed appropriate for the application as the accuracy at low pressure values would not be influential in reducing the formation of pressure ulcers.

6 Operating Interface

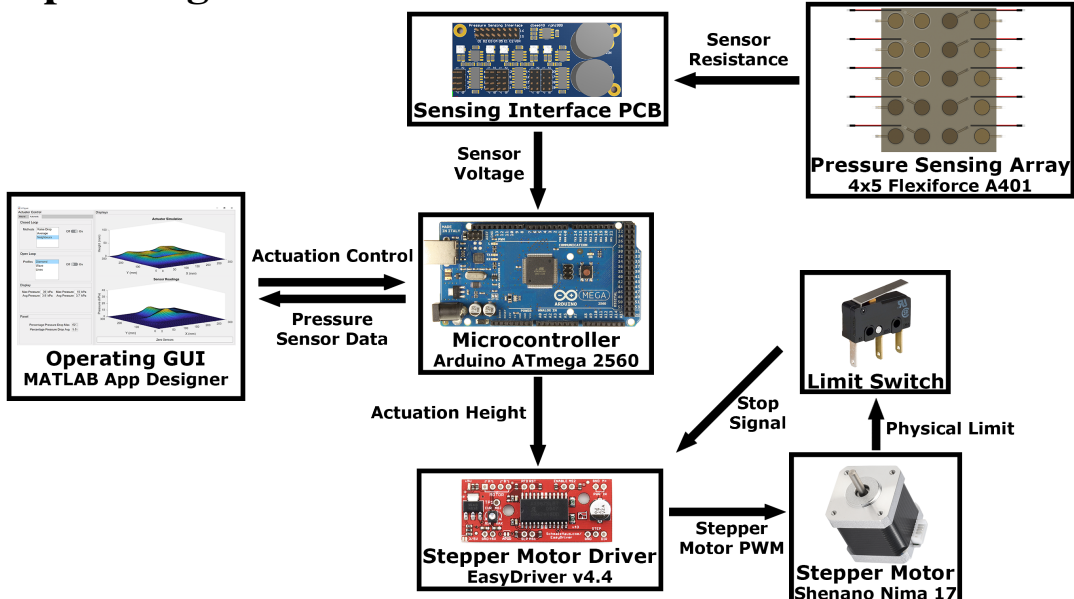


Figure 23: Soft Robotic Diagram Data Flow Diagram

The role of the operating interface is to process the sampled pressure sensor data from the Arduino ATmega 2560 microcontroller and return appropriate actuation control heights for each stepper motor based on the desired control selected by the operator. The information is processed and prepared in Matlab operating on a PC connected to the microcontroller via USB.

6.1 Communication

Serial communication protocols were used for transferring data between the PC and Arduino microcontroller, enabling a string of characters to be transmitted between the two ports. Actuation controls begin the string W to denote writing to the ATmega chip, followed by information for the desired height of each actuation module. Values are delimited by a space (' '), which is then decoded by the Arduino to update the stepper motors. Sensing information is requested from the Arduino by the PC by sending the letter 'R'. On arrival, pressure sensor values are composed into a string, also delimited by a space (' '). Example serial strings are demonstrated:

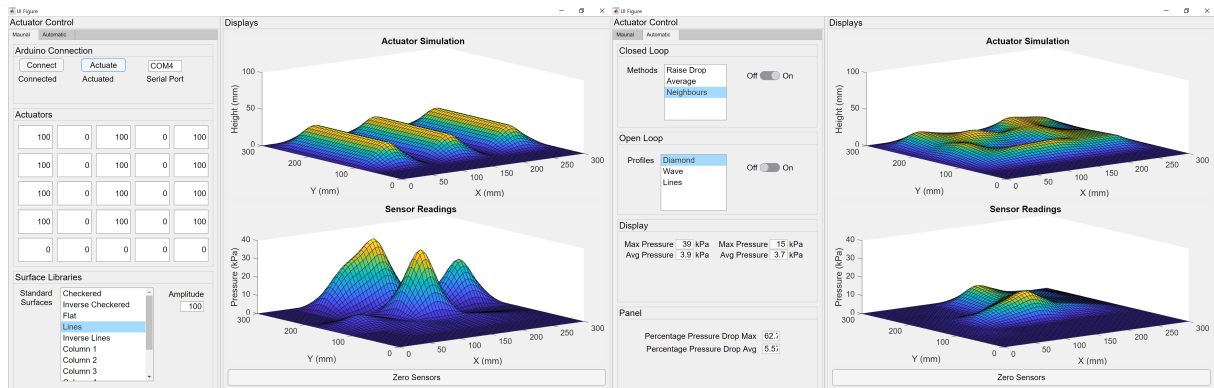
- **Pressure Sensor Data String:** send "R" return "17529 7908 ..."
- **Actuation Height Data String:** send "W 32 34 ..."

6.2 GUI

For the incoming pressure mapping information to be visually recognisable and allow for actuation heights to be simply defined, a GUI was developed to assist in the systems usability. The Matlab extension App Designer was used as the development framework for the controller interface. Key ideas of UI and UX were considered in the development to ensure the operation was clear and easy to follow.

The GUI demonstrated in Figure 24, consists of two main panels. The actuation control panel, residing on the left, houses two tabs for both manual and automatic modes of actuation. The manual tab allows the operator to initiate the serial connection with the Arduino board and to set custom actuation heights and update the surface via a button. A library of surface presets are provided at the bottom section of this panel to allow for common patterns to be quickly developed onto the array.

The automatic panel contains options for enabling control systems that uniquely adjust the actuator heights based on the selected method. Key pressure values summarised in the lower portion of the display, indicating the maximum and average pressure recorded on the surface.



(a) Manual Control GUI Example

(b) Automatic Control GUI Example

Figure 24: Operating System GUI

A 3D graphical plot of both the actuation surface and pressure distribution is represented on the right panel. Plots have been extrapolated into a surface distribution using the Makima interpolation method incorporated into the Matlab plot tool to obtain a smooth representation.

7 Control Logic

As demonstrated in section 6.2 on the operating interface, a series of actuation control methods were developed using both open-loop and closed-loop techniques.

7.1 Open Loop Control

Open-loop methods consist of a variety of cyclic patterns of actuation heights that aim to alternate the high pressure loading points regularly, similar to that used in the APAM's [5]. The cyclic motion inverses the pattern arrangement, lowering the high points and raising the low points. Patterns included in the operational modes include:

- **Diamond:** A checkerboard arrangement
- **Wave:** Produces a straight wave motion across the surface
- **Lines:** Straight parallel raised ridges and valleys (Figure 24a)

7.2 Closed Loop Control

Closed-loop methods incorporate the use of the sensing information as feedback to provide adjustments to the surface profile based on the current pressure distribution. The aims of the closed-loop control methods are to minimise the maximum interfacing loading pressure between the surface and the resting patient, increasing the area in which the load is spread across.

7.2.1 Average

The average method compares the pressure loading at each actuation location with the average pressure loading across the entire array as feedback to obtain an error. The respective actuator is then adjusted based on this error, using the proportional controller gain K . A control block diagram demonstrating two out of 20 of the total modules is demonstrated in Figure 25.

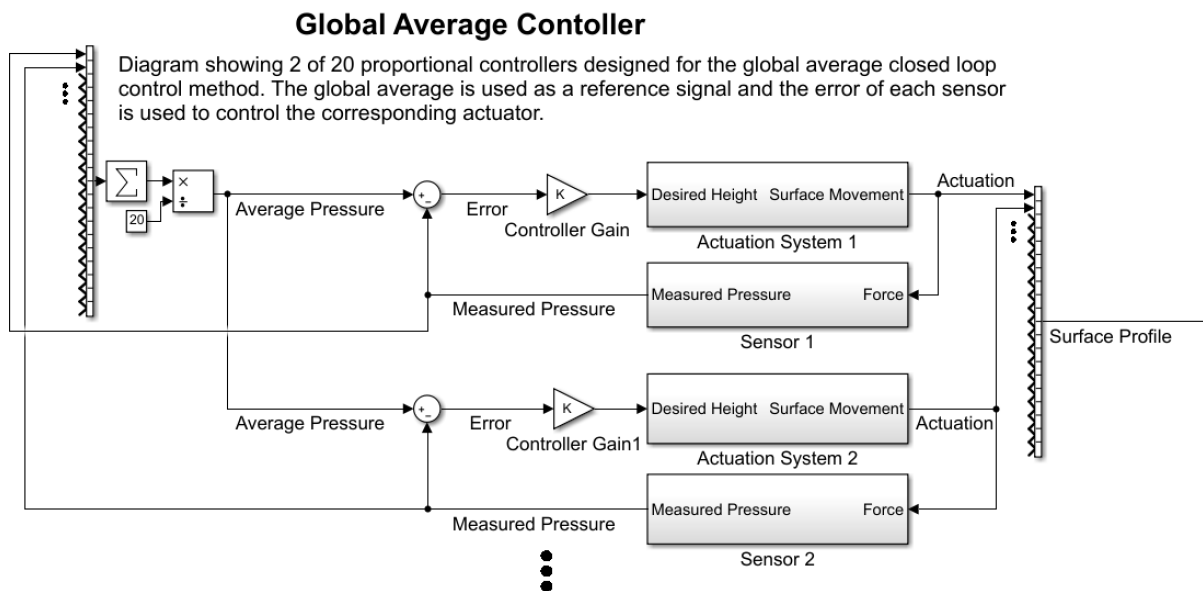


Figure 25: Average Controller Block Diagram

Due to data flow limitations in the serial communication between the PC and Arduino board, the discrete controller updates the actuator at a period of two seconds. Although, it would be an advantage to improve the operating frequency, it was deemed to not have a large enough influence on the systems ability to manage pressure ulcer development.

7.2.2 Localised Average

An issue identified with the average control method is that pressure from every other sensing node has an equal influence on the adjustment. In situations where the nodes directly surrounding the current node observe a drastic difference in pressure, while the rest of the array displays a similar value, the adjustment rate would be lower than desirable. An obvious solution to a slow settling time would be to increase the controller gain, however, this would result in larger overshoots and cause more disruption to the patient. Therefore, a localised average control method was developed.

The localised average control method aims to consider the relative pressure with the nearest neighbouring nodes when making actuation adjustments, rather than the full array. Additionally, a weighting is applied to each surrounding sensor sample relative to its distance from the reference position to favour the influence of closer nodes. To achieve this, when sampling the sensors S_{kl} in the pressure mapping array to adjust node N_{ij} , a distance D is calculated between their locations using equation 5. Figure 31b illustrates an example of the distance propagation through the array for N_{24} .

$$D = |(i - k)| + |(j - l)| \quad (5)$$

A function developed to take an array of sensing pressure data $Array$, a distance limit D_L , distance scalar D_s and controller gain K , has been included in Appendix B. This returns an array of actuation adjustments based on the localised average of the surrounding node samples S . Samples at a distance greater than D_L are excluded from the average and do not influence the adjustment. Surrounding samples less than or equal to D_L are inversely weighted by their distance from the actuation node, D_s varies this weighting as demonstrated in equation 6.

$$S_{Weighted} = \frac{S}{D \times D_s} \quad (6)$$

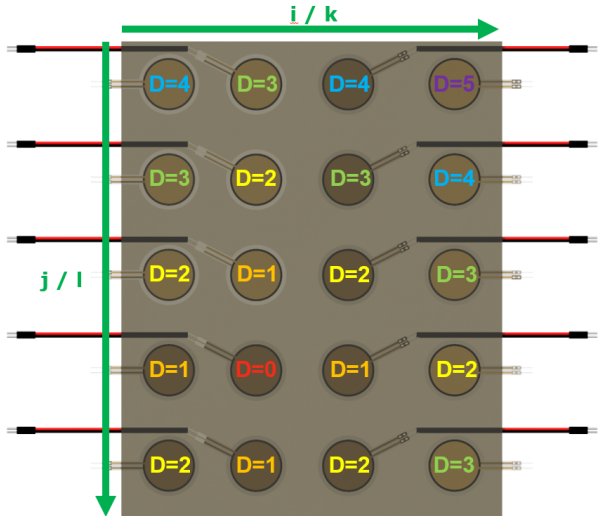


Figure 26: Sensing Array Distance Propagation

8 System Testing

8.1 Test Mannequin

To provide a complex and realistic pressure distribution for testing the performance of the pressure distributions, a 1:2 scale human mannequin was created. Using an online sourced 3D model of an adult human body [16], the portion of the body spanning from the sacral to upper thigh region was extracted. The front side of the model was flattened to allow weights to be safely applied to the model to adjust the resting mass. 3D-printing the model resulted in the a $60 \times 200 \times 240$ mm mannequin as presented in Figure 27.

8.2 Open Loop Control

8.2.1 Methodology

A mass of 10kg was applied to the top of the mannequin while it rested on the surface of the soft robotic mattress. Each method completed a complete pattern cycle at a height difference of 60mm between the raised and lowered nodes. Pressure mapping data were logged in Matlab to observe the average pressure distribution of the resting mannequin for each arrangement.

The performance of each method is evaluated based on the minimum pressure observed on each node for the two arrangements (inverse and non-inverse). This indicates each methods ability to periodically relieve the pressure distribution on each sensory position. As a lower magnitude of pressure exposure reduces the risk of developing pressure ulcers [1].



Figure 27: Mannequin

8.2.2 Results

Pressure distributions for the lines method are illustrated in Figure 28. Maximum pressure observed on both arrangements was 37kPa, while the minimum of the two was 19kPa.

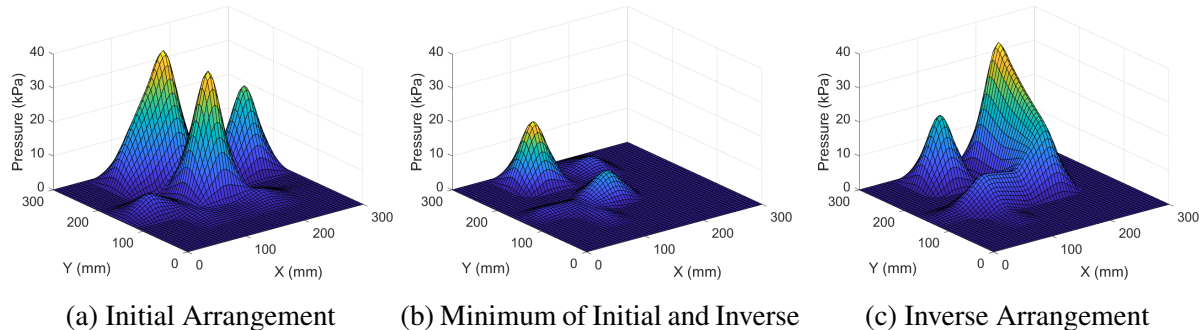


Figure 28: Pressure Distributions for Lines Method

Distributions for the diamond method are illustrated in Figure 29. Maximum pressure on the initial arrangement was 37kPa while 33kPa when inverted, with a combined minimum of 16kPa.

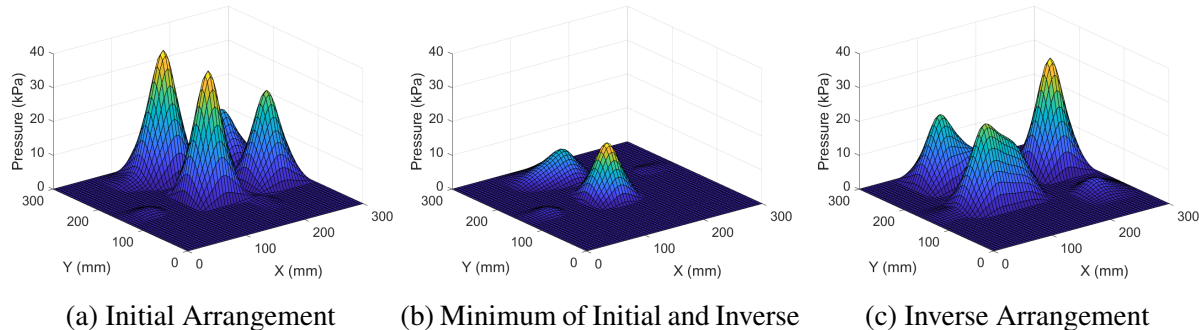


Figure 29: Pressure Distributions for Diamond/Checker Method

8.2.3 Discussion Open-loop

Both the lines and diamond methods displayed high pressure loading points above 30kPa in their respective initial and inverse arrangements. Sustained pressures at these levels are likely to develop pressure ulcers between 1-2 hours on susceptible patients [8]. The minimum observable pressure across the two arrangements in both methods reduced the pressure to less than 20kPa.

Demonstrating that both methods have the ability to redistribute the location of high pressure points using their respective cyclic patterns. This would extend the general development time of pressure ulcers from 1-2 hours to 2-3 hours.

8.3 Closed Loop

8.3.1 Methodology

Physical arrangements for the closed-loop methods were arranged in the same manner as in the open-loop test phase. The positioning of the weights and mannequin can be seen in Figure 30, demonstrating the testing setup.

The performance of the closed-loop methodologies is evaluated based on the maximum pressure observed on the pressure sensing array. With controls aiming to redistribute high loading points to surrounding areas, the maximum pressure reading should reduce at a rate proportional to the controller gain K . The average and localised average controllers are tested for a range of controller gains to determine their relative performance and optimal gains.

8.3.2 Results

Reduction in the initial maximum pressure point is demonstrated as a percentage in Figure 31 for both the average and localised average controller. The peak reduction from the average controller was 75% after 50 seconds of adjustment at a gain of $K = 0.25$, while the localised average controller achieved a reduction of 82% at a gain of $K = 1$.

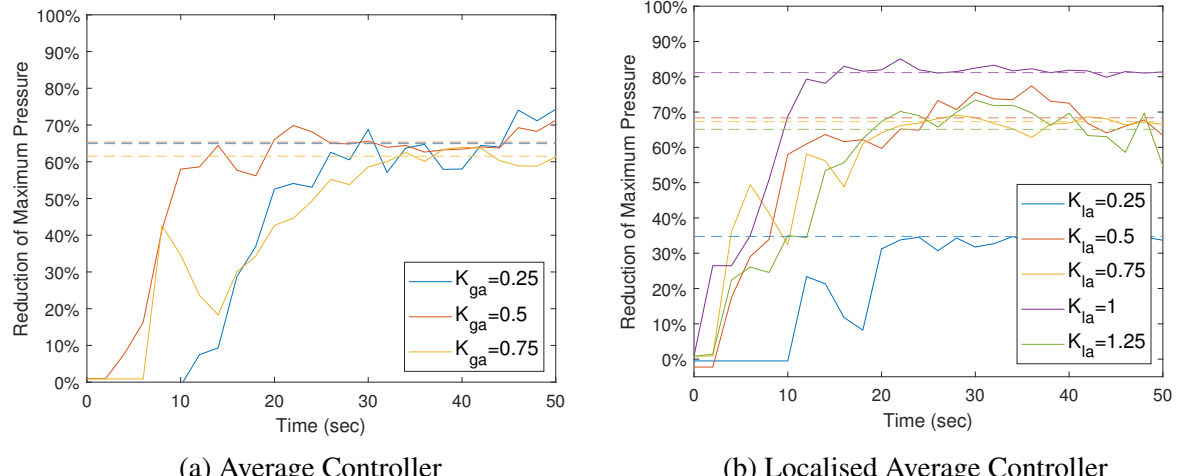


Figure 31: Maximum Pressure Reduction over Time

An example of the localised average controllers surface and actuation progression can be observed in Figure 32. As the surface gradually conforms the surface to redistribute the pressure distribution of the resting mannequin, the sensor profile smooths out to surrounding nodes.

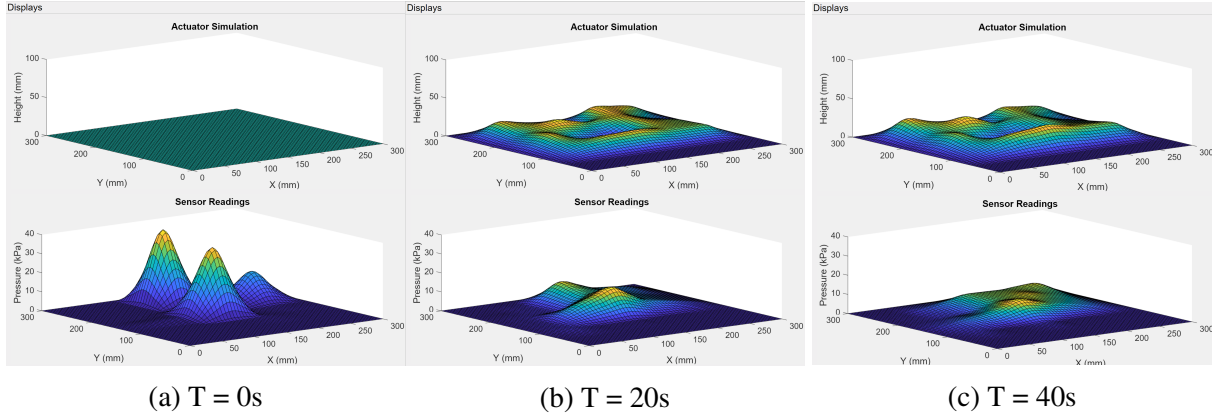


Figure 32: Actuation and Surface Profile Development for Localised Average Control

8.4 Discussion - Average Controller

Of the gains tested, $K = 0.5$ appeared to provide the optimal performance with a good balance of response time and stability in adjustments. The lower gain $K = 0.25$ achieved the largest reduction in pressure, although, was slow to respond. The higher gain $K = 0.75$ displayed large oscillations in pressure reduction, due to overshoots in the actuation adjustments made.

8.5 Discussion - Localised Average Controller

A gain of $K = 1$ performed the best, obtaining a pressure reduction of 82% within six adjustments ($T=12s$). Lower gains were unable to achieve comparable gains even after a running time of ($T=120s$), which is due to the adjustments becoming too small at low errors for the stepper motors to accurately perform. Larger gains tended to overcompensate in their actuation adjustments relative to the optimal and therefore causing oscillations in the reduction process.

8.6 Discussion - General Closed-loop

The optimal gain of the average controller is lower than that of the localised average controller due to the error sustaining a larger error. This is associated with a large portion of the sensory array not being loaded throughout the redistribution process, due to the test mannequin not resting above those nodes on the mattress. In the average control method, these unloaded portions of the sensory array continue to influence the control system, resulting in larger relative errors. To avoid drastic overshoots in actuation adjustments, the average controller can not sustain as large of a gain.

As brushed on in the localised average controller discussion, low gains are not able to achieve as strong of a performance. Due to friction in the actuation system, particularly the lead screw, very small adjustments are often not able to be performed accurately. When low errors are reached, low controller gains produce actuation adjustments that can not be carried out and therefore reach their optimal reduction prematurely. Larger gains would then in turn be desirable for prolonging the series of adjustments made.

Although, controller gains of an excessive magnitude cause the adjustments to overcompensate in correcting the observed error. Resulting in a large amount of unnecessary disturbance to the surface profile, which would be an uncomfortable and concerning experience for a patient. Large gains also have the potential to cause the controller to become unstable, however, because the pressure mapping values are bound between 0-40kPa is the design, this is not a major concern in the design. If future iterations were to extend the range of the pressure readings drastically, this should be considered.

9 Conclusions

An operable scale model of a soft robotic mattress has been created for the purpose of pressure ulcer prevention. Testing was carried out to assess the pressure reduction ability of a variety of control methods.

- **Actuation System:** A peristaltic table was repurposed to create a soft deformable surface that provided a method of pressure redistribution. Limit and electronic systems were repaired and overhauled to be more robust along with a new communication protocol.
- **Pressure Mapping:** A custom 4×5 array of piezoresistive sensors suspended in a flexible and stretchable elastomer. This created an interface for mapping the pressure distribution for a resting patient on the surface of the mattress.
- **Operational Interface:** An intuitive operating interface was created to handle communication between the physical components. Allowing control of the deformable surface, along with a virtual display of both actuation heights and pressure values.
- **Automatic Control:** Various control methods were explored with both open and closed loop methods. Demonstrating sophisticated pressure management capabilities for pressure ulcer prevention and management. The optimisation of proportional controller gains are optimised and discussed

The fully integrated system was tested using a scale mannequin and achieved pressure reductions of up to 81%. Drastically reducing the rate of pressure ulcer for susceptible patients.

10 Recommendations for Future Work

Although a successful system has been developed for use in pressure ulcer prevention and management, there are many future improvements that have been identified that would improve the operation.

- The development of a higher resolution sensing array would be advantages for the closed-loop control methods, with a more accurate representation of the pressure distribution.
- Sensor readings could be filtered to reduced the disturbance of noise and sudden variations in surface loading, creating smoother and more accurate actuation adjustments
- Moving the control logic processing from the PC to the Arduino microcontroller would drastically reduce the sampling time and controller update frequency.
- Feedback on the actuating stepper motors, such as an encoder, would guarantee the actuation heights of the soft robotic mattress. Ultimately improving the controllers accuracy and performance at low error situations.
- Relative performance of controller methods could be further explored to determine the optimal development parameters.
- A more realistic test mannequin could be developed to provide a better representation of the systems performance for patients.

References

- [1] M. Takahashi, J. Black, C. Dealey, and A. Gefen, “Pressure ulcer prevention. pressure, shear, friction and microclimate in context,” *Int Rev*, pp. 2–10, 01 2010.
- [2] L. E. Edsberg, J. M. Black, M. Goldberg, L. McNichol, L. Moore, and M. Sieggreen, “Revised national pressure ulcer advisory panel pressure injury staging system,” *Journal of Wound, Ostomy and Continence Nursing*, pp. 585–597, 11 2016.
- [3] M. Reddy, S. S. Gill, and P. A. Rochon, “Preventing pressure ulcers: a systematic review,” *JAMA*, vol. 296, no. 8, pp. 974–984, Aug 2006.
- [4] S. Zaratkiewicz, J. D. Whitney, J. R. Lowe, S. Taylor, F. O’Donnell, and P. Minton-Foltz, “Development and implementation of a hospital-acquired pressure ulcer incidence tracking system and algorithm,” *J Healthc Qual*, vol. 32, no. 6, pp. 44–51, 2010.
- [5] K. Vanderwee, M. Grypdonck, and T. Defloor, “Effectiveness of an alternating pressure air mattress for the prevention of pressure ulcers,” *Age and ageing*, vol. 34, pp. 261–7, 06 2005.
- [6] R. Behrendt, A. M. Ghaznavi, M. Mahan, S. Craft, and A. Siddiqui, “Continuous bedside pressure mapping and rates of hospital-associated pressure ulcers in a medical intensive care unit,” *American Journal of Critical Care*, vol. 23, no. 2, pp. 127–133, 2014. [Online]. Available: <http://ajcc.aacnjournals.org/content/23/2/127.abstract>
- [7] R. Philip, “Soft robotic mattress for pressure ulcer prevention and management,” *Part IV project partner report (ME040-2019)*, 2019.
- [8] A. Gefen, “Reswick and rogers pressure-time curve for pressure ulcer risk. part 1,” *Nursing Standard (through 2013)*, vol. 23, no. 45, p. 64, 2009.
- [9] T. V. Papakostas, J. Lima, and M. Lowe, “A large area force sensor for smart skin applications,” vol. 2, pp. 1620–1624 vol.2, June 2002.
- [10] E. Kwong and G. Pang, “Development of an intelligent seat for the alleviation of pressure ulcers,” in *2018 11th Biomedical Engineering International Conference (BMEiCON)*, Nov 2018, pp. 1–5.
- [11] R. Hashem. (2015) Design and development of a hybrid x-y peristaltic table. [Online]. Available: <https://researchspace.auckland.ac.nz/handle/2292/26296>
- [12] V. C. G. P. C. Stassi, S. Cauda, “Flexible tactile sensing based on piezoresistive composites: A review,” vol. 14, pp. 5296–5332, March 2014.
- [13] Tekscan. Flexiforce a401 piezoresistive sensor. [Online]. Available: <https://www.tekscan.com/products-solutions/force-sensors/a401>
- [14] ——. Best practices for electrical integration of the flexiforce sensor. [Online]. Available: https://www.tekscan.com/sites/default/files/BP%20-%20Electrical_Integration_FINAL.pdf
- [15] T. Instruments. Lm317l datasheet (rev.e). [Online]. Available: <http://www.ti.com/lit/ds/symlink/lm317l.pdf>
- [16] M. D. Arts. Free realistic adult male body 3d model. [Online]. Available: <https://www.turbosquid.com/3d-models/free-realistic-adult-male-body-3d-model/675179>

Appendix A: Arduino Loop Function

```
1 void loop()
2 {
3     // Loops through each potential multiplexer configuration,
4     // sampling an individual sensor from each of the 5 rows
5     for(int i = 0; i < 4; i++) {
6         // Reads the sensor interface input into ADC, assigning
7         // the voltage reading to the respective array storage
8         // location
9         SV[(i*5)+0] = (5.0*analogRead(INPIN0))/1023.0;
10        SV[(i*5)+1] = (5.0*analogRead(INPIN1))/1023.0;
11        SV[(i*5)+2] = (5.0*analogRead(INPIN2))/1023.0;
12        SV[(i*5)+3] = (5.0*analogRead(INPIN3))/1023.0;
13        SV[(i*5)+4] = (5.0*analogRead(INPIN4))/1023.0;
14        // The multiplexer control pins are then switched to
15        // cycle the current sensor interface connection
16        digitalWrite(CTRLPIN0, HIGH && (i & B00000001));
17        digitalWrite(CTRLPIN1, HIGH && (i & B00000010));
18        // Delay allows time for the switching signal to
19        // stabilise before the next set of samples are made
20        delay(10);
21    }
22    // Serial communication is updated to send sensory
23    // data to the control interface on the PC via USB
24    serial_read(sent);
25 }
```

Appendix B: Localised Average Controller Function

Program 1: Localised Average Controller

```
1 % localisedAverage.m: This function returns the weighted average of
2 % surrounding nodes with a specified limit.
3 %
4 % Inputs:
5 % Array - 2D array containing the values to be processed
6 %
7 % DL      - Represents the inclusive boundary distance at which samples
8 %             are taken around a given array node.
9 %
10 % Ds     - Distance scalar
11 %
12 % K      - Proportional controller gain
13 %
14 % Outputs:
15 % results- Array of height adjustments
16 function results = localisedAverage(app, Array, DL, Ds, K)
17
18     results = Array;
19     % For each actuating node in Array
20     [Ax, Ay] = size(Array);
21     for i=1:Ax
22         for j=1:Ay
23             samples = 0;      % Stores amount of samples made
24             samplesum = 0;    % Stores the sum of samples
25
26             for k=1:Ax
27                 for l=1:Ay
28                     % Calculates distance between actuating and sampling
29                     % node
30                     distance = abs(k-i) + abs(l-j);
31                     % Checks if sampling node is with the distance limit of
32                     % the actuating node and not the actuating node itself
33                     if (distance <= DL && distance~= 0)
34                         % Accumulates scale of samples made
35                         samples = samples + (1/(distance*Ds));
36                         % Accumulates the scaled sample value
37                         samplesum = samplesum + (Array(k,l)/(distance*Ds));
38                     end
39                 end
40             end
41             % Calculates the localised average of surrounding sampled nodes
42             samplesum = (samplesum/samples);
43             % Applies the adjusting gain to the error between the sample at
44             % the actuating node and the localised average
45             results(i,j) = round(K*(samplesum - Array(i,j)));
46         end
47     end
48 end
```

Appendix C: Altium PCB Schematic

